Progress In Electromagnetics Research C, Vol. 39, 179–192, 2013

MINIATURIZED WIDEBAND BANDPASS FILTER UTILIZING SQUARE RING RESONATOR AND LOADED OPEN-STUB

Kun Deng*, Jian-Zhong Chen, Bian Wu, Tao Su, and Chang-Hong Liang

National Laboratory of Science and Technology on Antennas and Microwaves, Xidian University, Xi'an, Shaanxi 710071, P. R. China

Abstract—In this paper, a miniaturized wideband bandpass filter utilizing a square ring resonator and loaded open-stubs is proposed. One pair of bent open-stubs characterized as perturbations is installed outside the diagonal corners of the ring, and another pair of loaded open-stubs is added inside the ring resonator. By stretching the perturbation stubs more than half-wavelength of the ring, three pairs of degenerated modes in a ring are split for wideband operation. The first two split modes form the dominant passband. Meanwhile, the loading effect introduced by the loaded open-stubs could move the third split mode into the dominant passband. At the same time, an additional transmission zero is generated by the loaded open-stub, which improves the skirt selectivity. Due to the applying of the perturbation stubs as long as more than half-wavelength, this kind of wideband microstrip ring resonator filter occupies a smaller size than those conventional ones that based on ring resonator. To verify the mechanism above, a wideband bandpass filter centered at 3.5 GHz is designed, implemented, and fabricated. Measured results of experimental circuit show good agreement with simulated responses.

1. INTRODUCTION

Wireless communication systems today make tremendous demands of compact high performance microwave bandpass filters (BPFs), ultra-wideband applications of information systems have promoted the development of wideband filter technology. Many different approaches have been developed for achieving wideband operation in wideband

Received 27 March 2013, Accepted 15 April 2013, Scheduled 28 April 2013

* Corresponding author: Kun Deng (dengkun139@gmail.com).

bandpass filters [1–11]. Stepped impedance resonators (SIRs) have been proved suitable for wideband applications due to their multi-mode characteristics [1–3]. Many other methods can also be used to design wideband BPFs. In [4], radial-line stubs were established to construct a multi-mode wideband BPF. Transversal signal-interaction concepts based on T-shaped structure can be seen in [5]. Ring/loop resonators were described in [6–11] and they have been paid more attention to because of their advantages such as small size, low loss. In [6], a pair of open-circuited stubs stretched close to one-eighth of a wavelength was loaded in a ring resonator, which made the first two even-order resonances move down to be quasi-equally located at two sides of the first odd-order resonance and thus forming a triple resonance ring resonator. Two extra resonances were moved into the passband when interdigital coupled lines were installed at two ports. In [7], a rectangular slot shape perturbation was excited to degenerate a dual mode, which generated two reject bands at each side of passband. Two one-quarter wavelength open stubs were added on the two sides of the ring to excite generation of bandstop response for controlling positions of transmission zero, achieving a sharp cutoff frequency characteristic. Dual stepped impedance stubs [8] were placed on the symmetrical plane of the feed lines with which the ring resonator was directly connected for wideband operation, this kind of wideband ring resonator BPF achieves 87% fractional bandwidth with a wide stopband bandwidth and sharp cutoff regions. A quadruple-mode ring resonator was developed in [9] by introducing a stepped impedance one-wavelength ring resonator into a stepped-impedance half-wavelength resonator, two band-stop sections with asymmetric π-type structure were introduced to suppress the harmonic responses for a wide stop-band. A single stepped impedance ring resonator was constructed to form wideband BPF with parallel-coupled feeder lines in [10]. In [11], a stepped impedance ring resonator was directly fed with a shunt open stub in between; half of the total ring path is coupled with the shut open stub. The shut stub along the coupled path generates triple resonances and results in a good passband flatness. Whatever, all the center frequencies of these conventional wideband microstrip ring resonator BPFs [6–11] center at the fundamental resonance of the ring resonator. As our best known, a ring is a full-wavelength resonator, thus the circuit sizes of these conventional wideband ring resonator BPFs are restricted by the circumference, i.e., the size of the ring. How to design a miniaturized wideband ring resonator BPF at the same center frequency is an attractive research topic.

This paper is aimed to solve the problem mentioned above, which can be seen as a good resolution in the design of miniaturized

wideband ring resonator BPFs. Detailed description on the operating principle of the wideband ring resonator BPF will be characterized in a comprehensive way by transmission line theory. The proposed filter with good frequency responses is found to center at a lower frequency than the fundamental resonance of the ring, thus having the smallest circuit size compared with those conventional wideband ring resonator bandpass filters.

2. FILTER DESIGN

2.1. Basic Theoretical Analysis

Figure 1(a) shows the schematic of the proposed wideband BPF. The initial wideband ring resonator is shown in Figure 1(b), it consists of one asymmetric square ring resonator and one pair of bent perturbation stubs. The two perturbation stubs are placed at two diagonal corners of the square ring. It is a symmetric structure, the symmetric plane is along the dashed line. With the even and odd mode excitations at two ports, the dashed line can be considered as a perfect magnetic wall or electric wall. Two of the half symmetrical resonators can be obtained, as shown in Figures 1(c) and (d), respectively. In Figure 1(b), θ_i ($i = 1$,

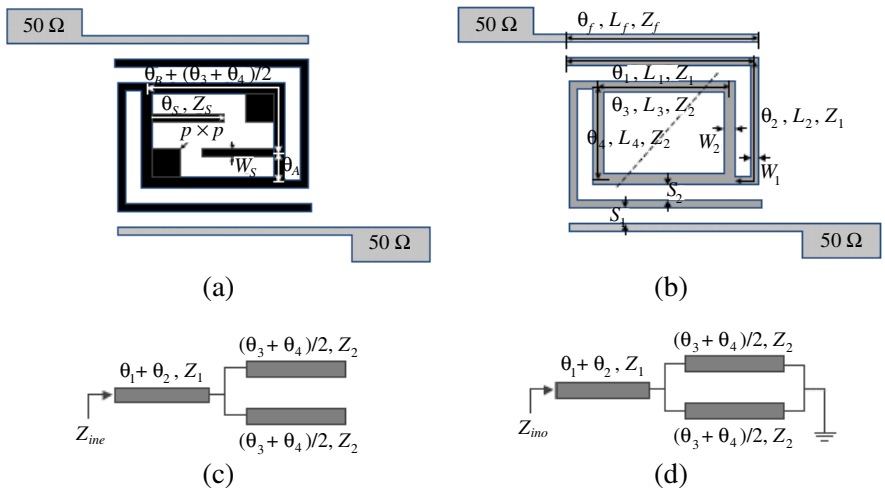

Figure 1. (a) Schematic of the proposed wideband ring resonator bandpass filter. (b) Initial structure of the wideband ring resonator bandpass filter. (c) Even mode of the equivalent circuit model. (d) Odd mode of the equivalent circuit model.

2, 3, 4) represents the electric length of each segment, L_i ($i = 1, 2, 3, 4$) is the physical length of θ_i. Z_1 and Z_2 are the impedances of the perturbation stub and the ring resonator, respectively. When even and odd mode motivate, the resonant frequencies can be obtained when the input admittances of even and odd modes, i.e., Y_{ine} and Y_{ino} are zero. The input impedances (Z_{ine} and Z_{ino}) and the resonant conditions have been derived in [12], for easy reading and understanding, the resonant conditions are listed below again:

$$2R_Z + \tan(\theta_1 + \theta_2) \cdot \cot[(\theta_3 + \theta_4)/2] = 0 \quad \text{for even mode} \quad (1)$$

$$2R_Z - \tan(\theta_1 + \theta_2) \cdot \tan[(\theta_3 + \theta_4)/2] = 0 \quad \text{for odd mode} \quad (2)$$

where $R_Z = Z_1/Z_2$.

Based on the resonant conditions, resonant frequencies of all the even and odd order modes can be solved through (1) and (2). For the special case of $Z_2 = 2Z_1$, the first two odd and the first even mode resonant frequencies can be deduced as follows,

$$f_{odd1} = \frac{c}{2(2L_1 + 2L_2 + L_3 + L_4)\sqrt{\varepsilon_{eff}}} \quad (3a)$$

$$f_{even1} = \frac{c}{(2L_1 + 2L_2 + L_3 + L_4)\sqrt{\varepsilon_{eff}}} \quad (3b)$$

$$f_{odd2} = \frac{3c}{2(2L_1 + 2L_2 + L_3 + L_4)\sqrt{\varepsilon_{eff}}} \quad (3c)$$

where c is the speed of the light in free space, and ε_{eff} denotes the effective dielectric constant of the substrate. From (3a)–(3c), we can find that $f_{even1} = 2f_{odd1}$ and $f_{odd2} = 3f_{odd1}$. For general case of arbitrary Z_2 and Z_1, variation of the resonant frequencies against different lengths of the perturbation stubs can be plotted according to (1) and (2).

Figure 2 plots the normalized resonant frequencies of the first two odd modes and the first even mode, f_{o1}/f_0, f_{o2}/f_0 and f_{e1}/f_o versus the length ratio of $k = (\theta_1+\theta_2)/(\theta_3+\theta_4)$ under the impedance ratio of $R_Z = 1$, where f_0 is the fundamental resonance of the ring resonator. For easy reading, we denote the three resonances, i.e., f_{o1}, f_{e1} and f_{o2}, as f_1, f_2 and f_3 in sequence. From Figure 2, it can be seen that, three resonant modes seem to be synchronously reduced as k increases and the three modes will be reduced lower than f_0 when $k > 1$. In the range of $k > 1$, the frequency separation of $f_2 - f_1$ is smaller than that of $f_3 - f_2$. Actually, f_1 and f_2 form the dominant passband and f_3 is far away from the passband. Figure 3(a) depicts the simulated frequency responses of one filter under weak and tight coupling cases, the simulations are done on a substrate with dielectric constant $\varepsilon_r = 2.65$ and thickness $h = 1\,\text{mm}$ (same as below). The

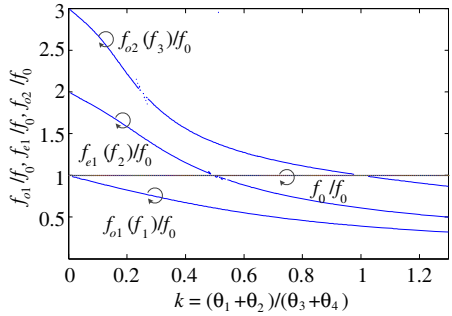

Figure 2. Normalized even and odd mode resonant frequencies versus normalized stub length.

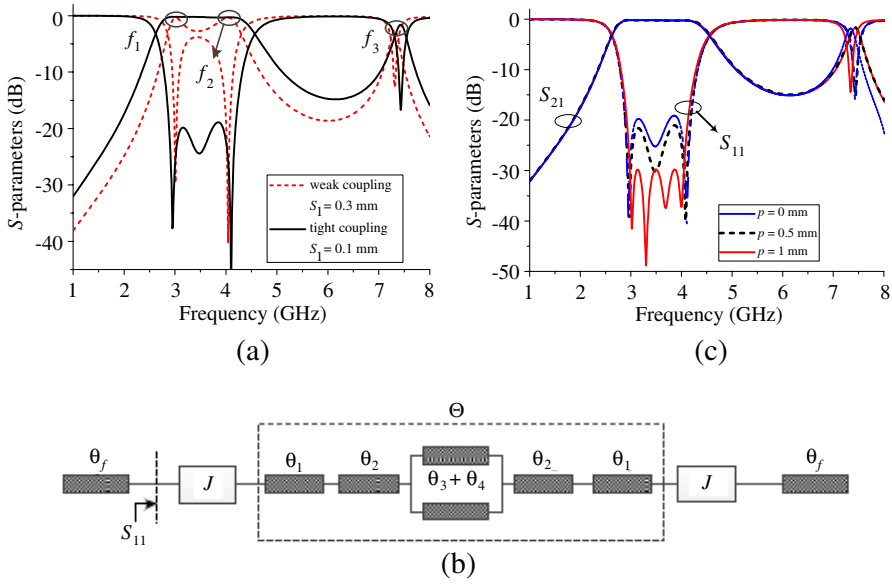

Figure 3. (a) Simulated frequency responses of the initial resonator under weak and tight couplings ($L_1 = 10.7\,\text{mm}$, $L_2 = 5.1\,\text{mm}$, $L_3 = 9.3\,\text{mm}$, $L_4 = 4.5\,\text{mm}$, $S_2 = 0.2\,\text{mm}$, $W_1 = 0.4\,\text{mm}$, $W_2 = 0.4\,\text{mm}$). (b) Equivalent circuit model of the initial resonator with an inverter. (c) Frequency responses against different patch sizes ($S_1 = 0.1\,\text{mm}$).

filter centers at 3.5 GHz and the fundamental resonant frequency (f_o) of the ring is about 8 GHz. The length ratio of k is about 1.2 and the impedance ratio of R_Z is 1. Apparently, the three resonant frequencies

are all reduced lower than the fundamental resonance f_0, and the first two resonant frequencies f_1 and f_2 form a wideband passband under a tight coupling.

From Figure 3(a), it can also be seen that there are 2 poles in the dominant passband formed by f_1 and f_2 under weak coupling ($S_1 = 0.3\,\text{mm}$) and another pole will be produced under tight coupling ($S_1 = 0.1\,\text{mm}$). The additional pole is caused by the parallel-coupled microstrip line (PCML) composed of the feeder line and the perturbation stub. To understand in depth of this, the reflection coefficient (S_{11}) is analyzed. Figure 3(b) plots the equivalent circuit of the initial filter in Figure 1(b). The PCML is expressed by two single transmission lines of electrical length θ_f, impedance Z_1 and admittance inverter parameter J. S_{11} is expressed as follows:

$$S_{11} = \frac{j\left(1-\bar{J}^4\right)\cdot\tan(\Theta)}{2\bar{J}^2 + j\left(1+\bar{J}^4\right)\cdot\tan(\Theta)} \tag{4}$$

where Θ is the equivalent electrical length of the resonator and $\bar{J} = J/Y_f$. From (4), each pole location where $|S_{11}| = 0$ can be found at the frequency: $\tan(\Theta) = 0$ or $\bar{J} = 1$. The first case corresponds to the resonant frequencies f_1, f_2 and f_3, which is determined by (1) and (2). The latter case is generated by extremely enhanced J-inverter susceptance. In this way, a multi-pole bandpass filter may be realized over a wide range from f_1 to f_2, if a tightly coupling degree can be achieved. In other words, there are at least two poles in the dominant passband formed by f_1 and f_2.

Additionally, the passband ripple can be easily optimized by adding two identical patches in another two diagonal corners of the ring, as shown in Figure 1(a). It has been known that, the second resonance (f_2) can be adjusted by tuning the patch size while the first resonance (f_1) changes little [12]. Figure 3(c) shows the simulated frequency responses of the initial resonator with different patch size p. From the figure, it can be seen that when the patch size increases from 0 to 1, the passband ripple can be equalized with magnitude of the return loss ($|S_{11}|$) reduced by 10 dB and 4 poles can be watched in the passband. As a result of this, tuning the patch size p could achieve a tight coupling for wideband operation, thus getting a good frequency response.

The attenuation out the right of the dominant passband is not satisfactory, which can be observed from Figure 3(c). In order to solve this problem, one pair of loaded open-stubs is installed inside the ring, as shown in Figure 1(a). The loading effect of the loaded open-stubs can shift the third resonance (f_3) downward without affecting the first (f_1) and the second resonance (f_2), meanwhile, the loaded open-stubs

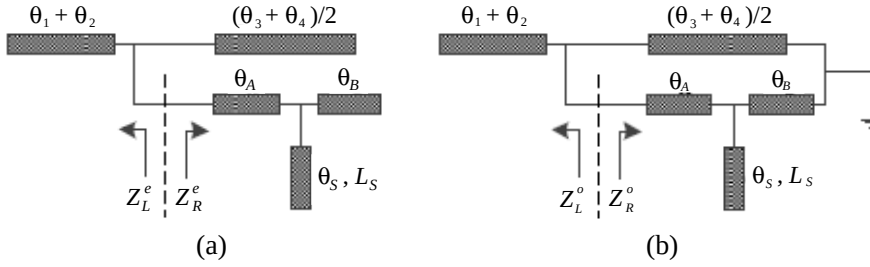

Figure 4. (a) Equivalent even mode circuit of the initial resonator with loaded open-stub. (b) Equivalent odd mode circuit of the initial resonator with loaded open-stub.

introduce a transmission zero at the right of the third resonance (f_3), which leads to a finely adjusted wideband passband performance.

Figure 1(a) shows the modified ring resonator with loaded open-stubs. Its simplified equivalent even and odd mode circuits are described in Figures 4(a) and (b). The resonant frequencies can be derived under the summation of input impedances ($Z_L^{e,o}$ and $Z_R^{e,o}$) be zero [6]. $Z_L^{e,o}$ and $Z_R^{e,o}$ are the input impedances looking into the left and right from the transverse, respectively. For the even mode, the resonant condition can be expressed as:

$$A_e + B_e = 0 \tag{5a}$$

where

$$A_e = R_Z R_S \cdot \tan\theta_B + R_Z \tan\theta_S - R_Z R_S \cdot \tan\theta_A \tag{5b}$$

$$\begin{aligned} B_e = {} & R_Z R_S \cdot \tan\left(\frac{\theta_3+\theta_4}{2}\right) + R_S \cdot \tan(\theta_1+\theta_2) \\ & + \tan\theta_A \cdot (R_S \cdot \tan\theta_B + \tan\theta_S) \cdot [\tan(\theta_1+\theta_2) \\ & + R_Z \cdot \tan\left(\frac{\theta_3+\theta_4}{2}\right)] \end{aligned} \tag{5c}$$

Similarly, the odd mode resonant condition can be derived as:

$$A_o + B_o = 0 \tag{6a}$$

where

$$\begin{aligned} A_o = {} & R_Z R_S \cdot \tan\left(\frac{\theta_3+\theta_4}{2}\right) - R_Z \cdot \tan\left(\frac{\theta_3+\theta_4}{2}\right) \\ & \cdot \tan\theta_B \cdot (\tan\theta_S - R_S \cdot \tan\theta_A) \end{aligned} \tag{6b}$$

$$B_o = R_S \cdot (\tan\theta_A + \tan\theta_B) \cdot \left[R_Z - \tan\left(\frac{\theta_3+\theta_4}{2}\right) \cdot \tan(\theta_1+\theta_2)\right] - \tan\theta_A \cdot \tan\theta_B \cdot \tan\theta_S \cdot \left[R_Z - \tan(\theta_1+\theta_2) \cdot \tan\left(\frac{\theta_3+\theta_4}{2}\right)\right] \quad (6c)$$

and $\theta_A + \theta_B = (\theta_3+\theta_4)/2$. When $\theta_S = 0$, $\theta_A = 0$ and $\theta_B = (\theta_3+\theta_4)/2$, the even mode resonant conditions of (5a)–(5c) will degenerate to (1) and the odd mode resonant conditions of (6a)–(6c) will degenerate to (2).

With arbitrary place of the loaded open-stubs, all the even and odd mode resonant frequencies can be determined by solving (5a)–(6c). On the other hand, the loaded open-stubs can be seen as a one-quarter wavelength resonator, which will introduce a transmission zero. The resonant condition for the transmission zero can be described as follows:

$$\cot\theta_S = 0 \quad (7)$$

Figure 5(a) plots the normalized resonant frequencies of the first three resonances (f_1/f_0, f_2/f_0 and f_3/f_0) and the transmission zero frequency (f_Z/f_0) versus the length ratio of $t = \theta_S/(\theta_3+\theta_4)$ under the fixed condition of $k = 1.2$, $R_Z = 1$, $R_S = 1$, $\theta_A = 0.1(\theta_3+\theta_4)$ and $\theta_B = 0.4(\theta_3+\theta_4)$. It can be found that, as t increases from 0 to 1, the third resonance (f_3) and the transmission zero frequency (f_Z) decrease fast simultaneously, yet the first two resonances (f_1 and f_2) retain almost unchanged. Keep increasing the loaded open-stubs, the third resonance (f_3) will be moved into the dominant passband. Meanwhile, a transmission zero is located at the right of the passband.

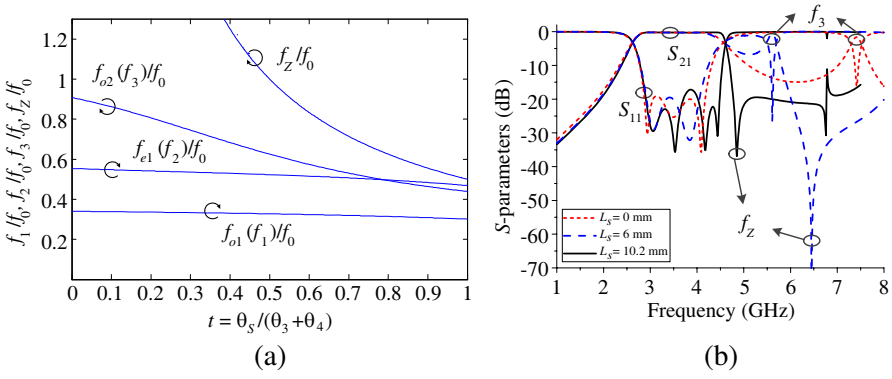

Figure 5. (a) Normalized resonant frequencies of the initial ring resonator with loaded open-stubs against different stub length. (b) Simulated frequency responses with different stub length ($p = 0$).

Figure 5(b) shows the simulated frequency responses of the three resonances (f_1, f_2 and f_3) and the transmission zero frequency (f_Z) versus different lengths (L_S) of the loaded open-stub. It can be found that when the loaded stubs are lengthened, the dominant passband has no change, the third resonance is moved into the passband, and a transmission zero is located tightly at the right of the passband. As a result of this, asymmetric sharp attenuation is obtained. Since the dominant passband is formed by f_1 and f_2, so we can suppose the center frequency (f_c) of the proposed wideband BPF is determined by the following equation:

$$f_c = \sqrt{f_1 \cdot f_2} \tag{8}$$

Moreover, the position where the loaded open-stubs should be located at is subjective, for there is always a suitable length of the loaded open stub to meet our design requirement.

2.2. I/O Coupling

The PCML is applied to meet the I/O coupling in our work. Closed-form function of the normalized $\bar{J}$ can be obtained by solving the equations below [13]:

$$\frac{Z_{oe}}{Z_1} = \frac{1 + \bar{J}\cos ec(\theta_f) + \bar{J}^2}{1 - \bar{J}^2\cot^2(\theta_f)} \tag{9a}$$

$$\frac{Z_{oo}}{Z_1} = \frac{1 - \bar{J}\cos ec(\theta_f) + \bar{J}^2}{1 - \bar{J}^2\cot^2(\theta_f)} \tag{9b}$$

where Z_{oe} and Z_{oo} are even and odd mode impedances of the coupled line of electrical length θ_f, the external quality factor Q is determined by

$$Q = \frac{\pi}{2} \cdot \frac{1}{\bar{J}^2} \tag{10}$$

Since Q is related with $\bar{J}$, while $\bar{J}$ is related with θ_f, Z_{oe} and Z_{oo}. Meanwhile, Z_{oe} and Z_{oo} are determined by the line width and the gap between two coupled microstrip lines [14], so we can conclude that the external quality factor Q can be adjusted by tuning θ_f, Z_f and S_1 according to (10).

2.3. Bandwidth

It has been known that a large impedance ratio of R_Z leads to a small frequency separation of $f_2 - f_1$, and vice versa [12]. Meanwhile, the center frequency of the proposed filter is determined by $\sqrt{f_2 \cdot f_1}$. Therefore, a large impedance ratio (R_Z) will generate a relatively

narrow fractional bandwidth (FBW), and a small impedance ratio will generate a wide FBW. Once the impedance ratio (R_Z) is fixed, the frequency ratio of f_2/f_1 will keep constant even though the normalized length ratio of k changes [12]. Consequently, the fractional bandwidth of the proposed filter will not change along with the variation of the length ratio (k) once the impedance ratio (R_Z) is fixed, which is beneficial for us during the filter design when we adjust dimensions to obtain precise center frequency.

Additionally, R_Z is determined by Z_1/Z_2, so the fractional bandwidth of the proposed filter can be modified by changing the line widths of the perturbation stubs and the ring resonator, i.e., W_1 and W_2.

2.4. Filter Design

According to the above analysis, the proposed wideband ring resonator BPF can be designed. For a given wideband filter specifications (f_c and FBW), the design procedure can be summarized as follows.

1) According to the FBW, select line widths of the ring resonator and the perturbation stubs so as to obtain the impedance ratio R_Z.
2) Choose a proper normalized electric length ratio k, the initial value should be select in the experiential range of $[1.2, 1.4]$.
3) Plot the normalized resonant frequencies versus normalized stub length according to (1) and (2).
4) Read the first two normalized resonant frequencies (f_1/f_0 and f_2/f_0) from the plotted figure at the certain position of k.
5) Calculate the fundamental resonance f_0 of the ring resonator according to the equation $f_0 = f_c/\sqrt{(f_1/f_0)\cdot(f_2/f_0)}$, and then obtain the wave-guided wavelength λ_0.
6) Define the initial dimensions of the filter, which should satisfy $L_3 + L_4 \approx \lambda_0/2$ and $(L_1 + L_2)/(L_3 + L_4) \approx k$.
7) Tune L_1, L_2, L_3, L_4 and W_2 to obtain accurate center frequency and FBW.
8) Add two loaded open-stubs to move the third resonance.
9) Adjust coupling length θ_f, line width W_f, and gap width S_1 to meet the external quality factor Q.
10) Add two patches and optimize the patch size p to get a good passband ripple.

3. RESULTS AND DISCUSSION

To verify the design principle, the filter centered at 3.5 GHz is fabricated on a substrate with dielectric constant $\varepsilon_r = 2.65$ and thickness $h = 1$ mm. Figure 6(a) depicts the photograph of the fabricated filter. Its optimized dimensions are: $L_1 = 10.7$ mm, $L_2 = 5.1$ mm, $L_3 = 9.3$ mm, $L_4 = 4.5$ mm, $L_A = 1.6$ mm, $L_B = 5.3$ mm, $L_S = 10.2$ mm, $S_1 = 0.1$ mm, $S_2 = 0.2$ mm, $W_1 = 0.4$ mm, $W_2 = 0.4$ mm, $W_S = 0.4$ mm, $p = 0.5$ mm. The measured and simulated results are indicated in Figure 6(b). Its measured center frequency is 3.5 GHz and its 3 dB fractional bandwidth is about 56.5%. The insertion loss is better than 0.86 dB and the return loss is greater than 14 dB. The attenuation rate for the sharp attenuation is about 134.5 dB/GHz (calculated from 4.61 GHz with 2.99 dB to 4.85 GHz with 35.2 dB), which greatly improve the skirt selectivity.

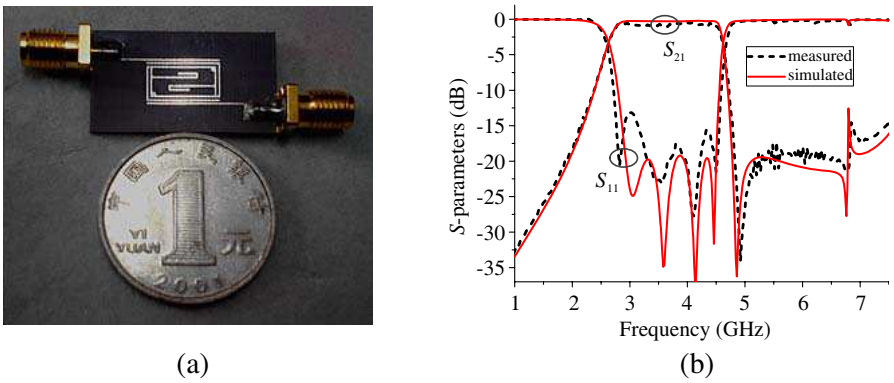

Figure 6. (a) Photograph of the fabricated filter. (b) Comparison of the simulated and measured results of frequency responses.

Table 1 compares the circuit size of the filter in this paper with those in [6–11]. λ_c is the wave-guided length of the filter at center frequency. It can be found that, the filter in this work has obvious advantage in miniaturization of the wideband microstrip ring resonator BPFs than those utilizing conventional structures. The reason is that the center frequency of the proposed filter is lower than the fundamental resonance of the ring, while conventional wideband microstrip ring resonator BPFs usually center at the fundamental resonance of the ring. As a result of this, the proposed filter occupies a smaller circuit size than those conventional filters do under the normalized frequency.

Take for example, the wave-guided length at 3.5 GHz is 60.8 mm, if

Table 1. Comparison of the wideband microstrip ring resonator BPFs.

Wideband bandpass filter	Substrate	Center frequency (GHz)	FBW (3 dB)	Size ($\lambda_c \times \lambda_c$)
Figure 9(b) in Ref. [6]	$\varepsilon_r = 10.8$, $h = 0.635\,\text{mm}$	4.2	64%	0.41×0.41
Figure 7 in Ref. [7]	$\varepsilon_r = 3.2$, $h = 0.762\,\text{mm}$	5	52%	0.85×0.85
Figure 5 in Ref. [8]	$\varepsilon_r = 6.15$, $h = 0.635\,\text{mm}$	2.5	87.3%	0.73×0.4
Figure 1 in Ref. [9]	$\varepsilon_r = 11.2$, $h = 1.6\,\text{mm}$	1.45	57.9%	0.77×0.13
Figure 1 in Ref. [10]	$\varepsilon_r = 9.8$, $h = 1.27\,\text{mm}$	2	30%	0.27×0.27
Figure 8 in Ref. [11]	$\varepsilon_r = 4.55$, $h = 0.8\,\text{mm}$	1.02	29.36%	0.41×0.48
Figure 6(a) in this paper	$\varepsilon_r = 2.65$, $h = 1\,\text{mm}$	3.5	56.5%	0.18×0.1

we use the conventional structures to construct a wideband microstrip ring resonator BPF, the center frequency will locate at the fundamental resonance of the ring, and the ring is a full-wavelength resonator. Therefore, size of the ring will be at least $(60.8/4) \times (60.8/4) = 231.04\,\text{mm}^2$. If we use the structure proposed in this paper, we can find that the size of the ring can be reduced as

$$\frac{231.04 - 9.3 \times 4.5}{231.04} \approx 81.89\%$$

Consequently, the proposed wideband microstrip ring resonator BPF has the smallest circuit size compared with those conventional ones at the same center frequency.

4. CONCLUSION

A miniaturized wideband microstrip ring resonator bandpass filter has been presented in this paper. More than half-wavelength perturbation stubs are utilized to form a wideband passband. Loaded open-stubs are used to obtain a good out-of-band performance, and square patches are added to get a better passband ripple. Detailed working principle and design procedure are demonstrated to construct this kind of filter.

Results indicate that the filter has a very attractive advantage of compact size. Measured results agree well with simulated ones.

ACKNOWLEDGMENT

This work was supported by the National High Technology Research and Development Program of China (863 Program) No. 2012AA01A308 and the National Natural Science Foundation of China (NSFC) under Project Nos. 61271017 and 61072017.

REFERENCES

1. Chen, L., F. Wei, X.-W. Shi, and C.-J. Gao, "An ultra-wideband bandpass filter with a notch-band and wide stopband using dumbbell stubs," *Progress In Electromagnetics Research Letters*, Vol. 17, 47–53, 2010.
2. Deng, H.-W., Y.-J. Zhao, L. Zhang, X.-S. Zhang, and W. Zhao, "Compact wideband bandpass filter with quadruple-mode stub-loaded resonator," *Progress In Electromagnetics Research Letters*, Vol. 17, 125–132, 2010.
3. Krongkitsiri, W., C. Mahatthanajatuphat, and P. Akkaraekthalin, "Wideband bandpss filters using parallel-coupled SIRs with wide spurious suppression," *Progress In Electromagnetics Research C*, Vol. 27, 69–83, 2012.
4. Zhang, L., Z.-Y. Yu, and S.-G. Mo, "Novel planar multimode bandpass filters with radial-line stubs," *Progress In Electromagnetics Research*, Vol. 101, 33–42, 2010.
5. Xue, S., W. Feng, H. Zhu, and W. Che, "Microstrip wideband bandpass filter with six transmission zeros using transversal signal-interaction concepts," *Progress In Electromagnetics Research C*, Vol. 34, 1–12, 2013.
6. Sun, S. and L. Zhu, "Wideband microstrip ring resonator bandpass filters under multiple resonances," *IEEE Trans. Microw. Theory Tech.*, Vol. 55, No. 10, 2176–2182, Oct. 2007.
7. Ahonnom, S. and P. Akkaraekthalin, "Wideband dual mode microstrip bandpass filters using a new perturbation with notch rectangular slots," *Proceeding of ECTI-CON*, Vol. 1, 269–272, 2008.
8. Kim, C.-H. and K. Chang, "Wideband ring resonator bandpass filter with dual stepped impedance stubs," *IEEE MTT-S Int. Microw. Symp. Dig.*, 229–232, May 2010.

9. Fan, J., D.-Z. Zhan, C.-J. Jin, and J.-R. Luo, "Wideband microstrip bandpass filter based on quadruple mode ring resonator," *IEEE Microw. Wireless Compon. Lett.*, Vol. 22, No. 7, 348–350, Jul. 2012.
10. Ma, Z.-W., H. Sasaki, C.-P. Chen, T. Anada, and Y. Kobayashi, "Design of a wideband bandpass filter using microstrip parallel-coupled dual-mode ring resontaor," *Asia-Pacific Microwave Conference Proceedings*, 21–24, Dec. 2010.
11. Srisathit, K., A. Worapishet, and W. Surakampontorn, "Design of tripple-mode ring resonator for wideband microstrip bandpass filters," *IEEE Trans. Microw. Theory Tech.*, Vol. 58, No. 11, 2867–2877, Nov. 2010.
12. Deng, K., S. Yang, S.-J. Sun, B. Wu, and X.-W. Shi, "Dual-mode dual-band bandpass filter based on square loop resonator," *Progress In Electromagnetics Research C*, Vol. 37, 119–130, 2013.
13. Makimoto, M. and S. Yamashita, "Bandpass filters using parallel coupled stripline stepped impedance resonators," *IEEE Trans. Microw. Theory Tech.*, Vol. 28, No. 12, 1413–1417, Dec. 1980.
14. Hong, J.-S. and M.-J. Lancaster, *Microstrip Filters for RF/Microwave Applications*, John Wiley & Sons, Inc., 2001.